TABLE 9 Characteristics of the composition of sediment sampled from different elements of the ripples (by "Shkorpilovtzy-83" experimental data)

Date	h m	Sampled part of rippple	$\bar{d}$ mm	γ_v %	K_a	K_E
10 Nov	3.5	Crest	0.23	28.4	–0.75	0.99
		Upper slope	0.23	27.3	–0.67	1.15
		Trough	0.20	24.3	–0.58	1.57
2 Nov	5.0	Crest	0.25	26.1	–0.47	0.62
		Upper slope	0.24	25.8	–0.44	0.65
		Lower slope	0.23	25.0	–0.47	0.78
		Trough	0.23	24.9	–0.57	0.83
10 Nov	16.0	Crest	0.82	204.8	0.28	0.34
		Upper slope	0.83	206.2	0.13	0.56
		Lower slope	0.90	392.5	–0.11	0.84
		Trough	0.96	461.6	–0.52	–0.87
2 Nov	18.0	Crest	0.73	125.2	–0.38	0.74
		Upper slope	0.72	106.8	–0.25	1.75
		Lower slope	0.81	202.1	–0.81	1.49
		Trough	1.00	1146.2	–0.42	–0.33

accumulate around the pile. Further from the pile, the turbulence decreases, and suspended particles which saturate the flow settle on the sea floor. Thus, the mean size of sand grains is relatively low here. At a distance exceeding three diameters of the pile, additional turbulence of the water mass becomes insignificant and the presence of the pile does not affect the bed sediment composition.

5.4 Conditions for active ripple existence

It was noted in Chapter 2 that in engineering practice critical velocities are frequently evaluated by a formula such as equation (2.2). It is sometimes used for determination of ripple existence conditions (Murina and Halfin, 1981). The range of ripple existence verified by the data of field observations is graphically shown in Fig. 66. The results of bedform studies in marine nearshore (Inman, 1957; Miller and Komar, 1980a; Nielsen, 1984) and lake zones (Tanner, 1971) were also used for comparison. Inman's observation data (Inman, 1957) are taken from the graphics given in Miller and Komar (1980a) and Nielsen (1981). Only the results obtained in unambiguously deciphered conditions were used.

TABLE 10 Characteristics of sediment composition at various distances from a pile (results from the "Shkorpilovtzy-83" experiment)

Date	h m	Distance from pile	$\bar{d}$ mm	γ_v %	K_a	K_E
4 Nov	3.5	0	0.66	169.1	–0.22	–0.70
		10	0.31	35.5	–0.52	0.22
6 Nov	2.6	0	0.49	80.2	–0.42	–0.19
		10	0.21	24.6	–0.95	2.59
18 Nov	3.1	0	0.31	28.1	–0.29	0.61
		0.5	0.21	20.7	–0.70	2.22
		3	0.28	20.3	–0.47	1.16
		6	0.28	23.7	–0.28	0.85
		9	0.27	22.8	–0.55	0.41

Tanner (1971) also made marine observations under a calm sea when maximal near-bottom velocities were obviously less than those necessary for initiation of particle movement. In this case only relic ripples were observed; thus, Tanner's data were not used in the present study. Dingler's experimental points corresponding to extremely small ripples (Dingler, 1974) were not used either because of high determination errors. Experimental data from Miller and Komar (1980a) were chosen in accordance with their recommendations. The range of variation measured and calculated parameters taken from observation data are tabulated in Table 11. Amplitude values of near-bottom orbital velocities during ripple observations were calculated in accordance with linear wave theory. In all the comparisons, values of "significant" orbital velocities were used, calculated by heights of the average waves among one-third of the largest waves. In accordance with available estimates (Kos'yan, 1984; Miller and Komar, 1980a; Nielsen, 1981), characteristics of these waves determine the nature of sediment motion under an irregular sea. With the use of these parameters, results of natural observations can be compared with laboratory results obtained under monochromatic waves.

It is evident from Fig. 66 that the data of the field observations do not go beyond the beginning of ripple formation as suggested by Murina and Halfin (1981). U_{cr} curves corresponding to ripple flattening disagree with the observed results. The majority of experimental points suggested by all the authors and proving the existence of ripples under given conditions, lie above the boundary corresponding to the beginning of the "smooth phase" of sediment movement.

The criteria of ripple existence suggested by Brebner (1980) and Dingler (1974) and discussed in Chapter 2, can be written in the form of (2.2). Quartz

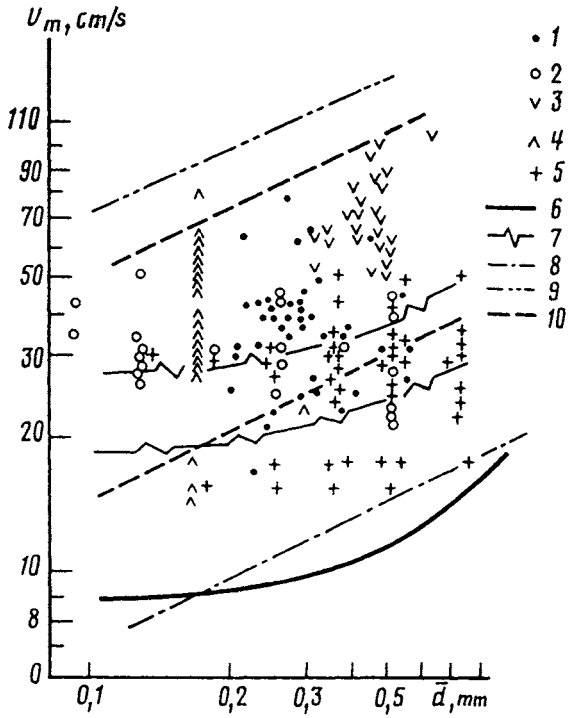

FIGURE 66 Comparison of field observation data of (1) Kos'yan (1985); (2) Inman (1957); (3) Miller (1980a); (4) Nielsen (1984); (5) Tanner (1971) with various relationships restricting the range of ripple existence; (6) initiation of ripple formation, after Murina and Halfin (1981); (7) lower and upper boundaries of initiation of smooth bottom zone formation, after Murina and Halfin (1981); relationships of (8) initiation of ripple formation (Brebner, 1980); (9) ripple disappearance (Dingler, 1974); (10) limiting curves for the range of ripple existence (Vongvisessomjai, 1984).

sands ($\rho_s = 2.65$ g cm^{-3}) have a range of U_m values, delimiting the area of the existence of ripples in the wave flow

$$\text{from } U_m = 2.2\sqrt{gd} \text{ to } U_m = 19.9\sqrt{gd} \tag{5.1}$$

Vongvisessomjai (1984) suggested a narrower range:

$$\text{from } U_m = 4.6\sqrt{gd} \text{ to } U_m = 14.4\sqrt{gd} \tag{5.2}$$

TABLE 11 Variation ranges of surface wave and bed microform parameters

Condition	h m	$\bar{d}$ mm	$\bar{T}$ s	λ_r cm	H_r cm	Author
Field	0.7–18.0	0.08–1.45	2.7–6.3	5.0–300.0	0.5–50.0	Kos'yan, 1985
	–	0.09–0.50	0.7–13.0	7.8–90.0	0.6–14.8	Inman, 1957
	3.1–21.3	0.17–0.29	6.0–18.2	7.6–27.1	–	Miller, Komar 1980a
	1.3–1.8	0.11–0.61	5.7–12.9	35.0–80.0	4.3–15.0	Nielsen, 1984
	0.2–0.6	0.13–0.71	0.8–6.2	3.5–14.6	0.5-3.4	Tanner, 1971
Laboratory	0.1–0.5	0.20–0.30	1.0–1.5	6.5–24.0	1.5–5.5	Keremetchiev (personal communication)
	0.6–0.7	0.24	1.8–2.4	16.0–18.0	4.0–5.0	Antsyferov et al., 1977
	–	0.28–1.06	1.9–10.1	4.6–33.6	0.1–1.9	Manohar, 1955
	0.3	0.17	3.0–5.0	13.0–16.0	–	Miller, Komar 1980b
	0.4	0.08–0.55	1.0–1.7	2.5–16.6	0.41–2.7	Nielsen, 1979

Having compared the above conditions for the existence of ripples to the data from field studies (Fig. 66), one can easily see that the latter criterion is not fulfilled as a great number of experimental points lie beyond the limits of ripple existence. At the same time, the greater part of natural observation results remain in the range (5.1) which can be used for a rough evaluation of the conditions for ripple formation and flattening.

All the above criteria for the existence of ripples due to wave flow differed from similar criteria for steady flow only in that the maximum value of near-bottom orbital velocity was taken into account instead of steady near-bottom current velocity. It has been shown in Chapter 2 that for correct description of bottom particle behavior, wave period influence should be accounted for (Dingler, 1979; Komar and Miller, 1975; Vongvisessomjai, 1984). Formulas suggested by these authors have been tested; the results are shown in Figs. 67 and 68. Equation (2.33) corresponding to wave conditions at the beginning of

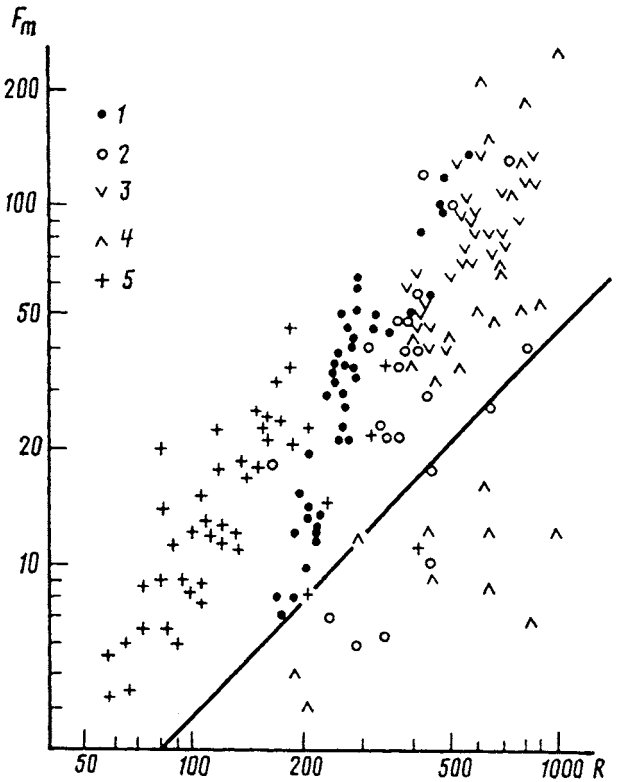

FIGURE 67 Comparison of field observation data with Dingler's relationship (2.27) (Dingler, 1979). For legend, see Fig. 66.

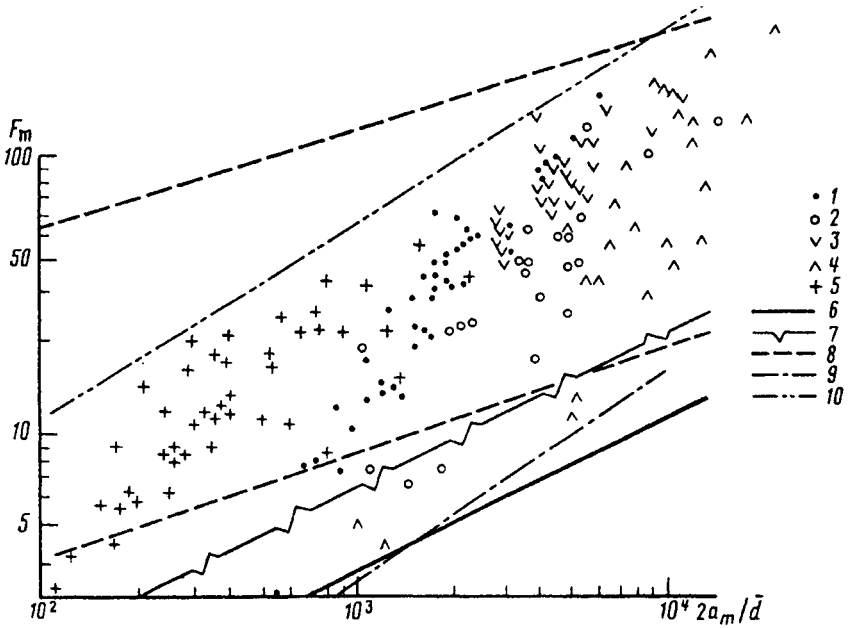

FIGURE 68 Comparison of field data with initial conditions of ripple formation (after Komar and Miller, 1975) (6); initiation of developed ripple (Komar and Miller, 1975) (7); limiting conditions for ripple existence (Vongvisessomjai, 1984) (8); (9) equation (5.31); (10) equation (5.4); (1)–(5) as in Fig. 66.

ripple formation on an erodible bottom, is confirmed by all the observed data. A significant amount of data obtained by various authors do not fit the conditions for the presence of ripples suggested by Vongvisessomjai (1984). Dingler's formula (Dingler, 1979) is the closest to the test points, but it is not supported by some of the observed results.

The set of data on the existence of ripples in the sea (Fig. 68) can be limited in a most efficient manner by the range of conditions found empirically (Kos'yan, 1987).

$$F_m = 3.3 \cdot 10^{-2} \left(\frac{2a_m}{\bar{d}} \right)^{2/3} \tag{5.3}$$

$$F_m = 5.4 \cdot 10^{-1} \left(\frac{2a_m}{\bar{d}} \right)^{2/3} \tag{5.4}$$

It should be noted that for silty sediments the curve given by equation (5.4) approximates Dingler's curve (Dingler, 1979).

The experimental points in Fig. 68, corresponding to the existence of ripple conditions, all lie within a confined area while the above criteria in equations (5.3) and (5.4) border this field only partially. Thus, combining the criteria suggested by different authors and favorably verified by observed data, one can get the range of existence of bottom sand microform.

First, let us compare the chosen criteria with the laboratory experiments published in a number of studies—Antsyferov et al., 1977; Nielsen, 1979; Miller and Komar, 1980b; and Manohar, 1955. The results of this comparison are shown in Fig. 69. Ranges of laboratory parameters are given in Table 11.

Combining conditions (5.4) and (5.5) with the above criteria of Brebner (1980) and Dingler (1974) and allowing for all the experimental points to lie within a range of $2a_m/\bar{d}$ from 100 to 5000, the conditions for ripple existence can be written in F_m and $2a_m/\bar{d}$ coordinates:

$$3 \leq F_m \leq 240 \tag{5.5}$$

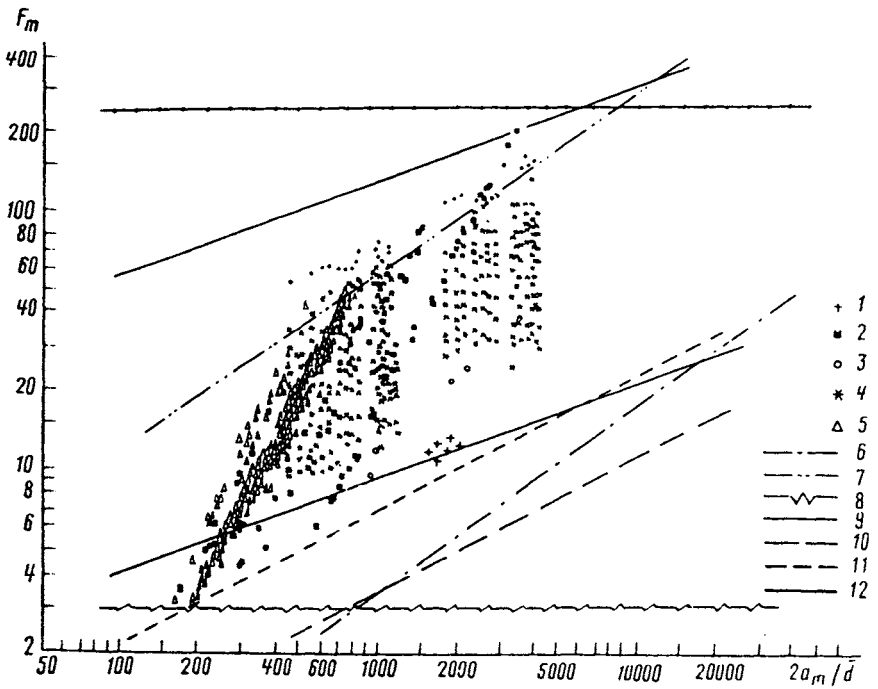

FIGURE 69 Comparison of laboratory data with conditions limiting the range of ripple existence. (1) Antsyferov et al., 1977; (2) Nielsen, 1979; (3) Miller and Komar, 1980b; (4) Manohar, 1955; (5) Keremetchiev (unpublished data); (6) equation (5.3); (7) equation (5.4); (8) Brebner, 1980; (9) Dingler, 1974; (10, 11) Komar and Miller, 1975; (12) Vongvisessomjai, 1984.

$$F_m = 3.3 \cdot 10^{-2} \left(\frac{2a_m}{\bar{d}} \right)^{2/3} \tag{5.6}$$

$$F_m = 5.4 \cdot 10^{-1} \left(\frac{2a_m}{\bar{d}} \right)^{2/3} \tag{5.7}$$

$$100 \leq \frac{2a_m}{\bar{d}} \leq 25{,}000 \tag{5.8}$$

Conditions for wave ripple existence based on the Shields parameter (Nielsen, 1981; Komar and Miller, 1975) are compared with field observation data with the results presented in Fig. 70, which clearly shows that these authors' criteria are roughly equivalent and mostly agree with the observed data.

Universal conditions of bed microform existence, allowing for the influence of wave period and bottom roughness, can be obtained in Ψ, $2a_m/\bar{d}$ coordinates. All the experimental points obtained in laboratory and natural conditions are shown in Fig. 71.

An attempt to contour the entire field of experimental points by an ellipsis equation (Fig. 71) seems to be more correct:

$$1 = \frac{\left[-5.80 + 0.88 \ln(2a_m/\bar{d}) + 0.47 \ln \Psi \right]^2}{8.41} + \frac{\left[5 - 0.47 \ln(2a_m/\bar{d}) + 0.88 \ln \Psi \right]^2}{1.69} \tag{5.9}$$

which can be simplified and reduced to

$$0.23 \ln(2a_m/\bar{d}) - 0.26 \ln \Psi + 0.06 \ln(2a_m/\bar{d}) \ln \Psi - \left[0.11 \ln(2a_m/\bar{d}) + 0.17 \ln \Psi \right]^2 = 1 \tag{5.10}$$

5.5 Active ripple parameters

The results of our measurements of active ripple parameters were compared with those calculated with equations (2.21)–(2.23). Graphical representations

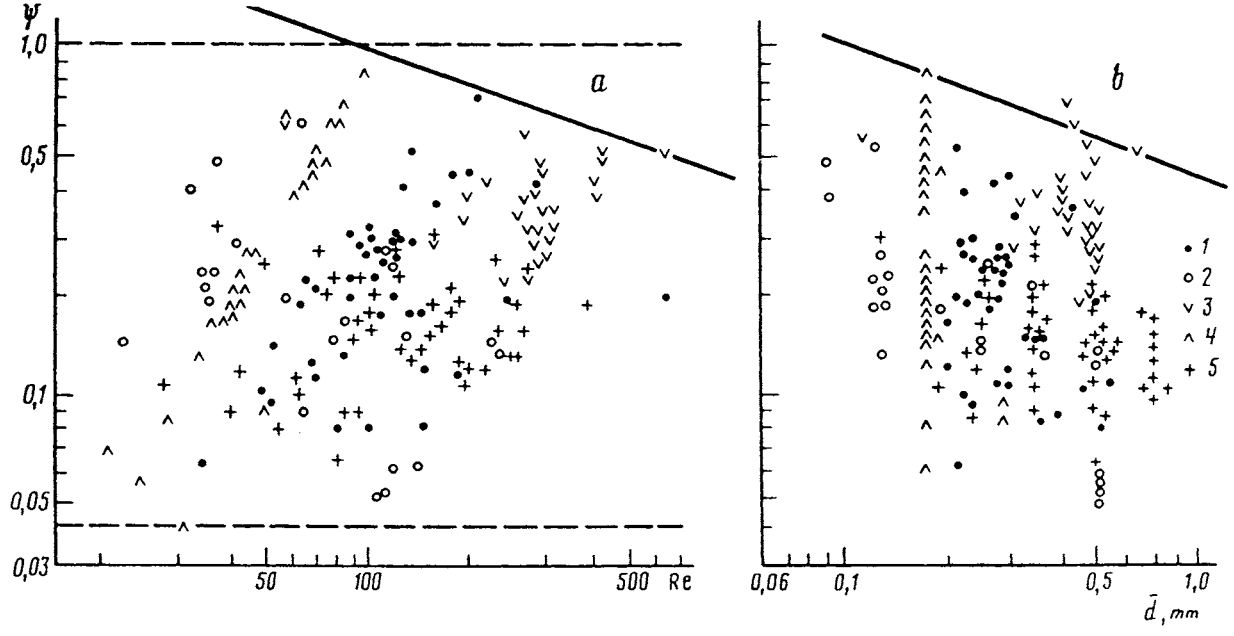

FIGURE 70 Ripple disappearance conditions in relation to Reynolds number (a) and mean bed sediment diameter (b). 1–5 see in Fig. 66. The range of values for Shields parameter suitable for ripple existence is shown by a dashed line (after Nielsen, 1981); the solid line delineates the conditions of ripple disappearance (after Komar and Miller, 1975).

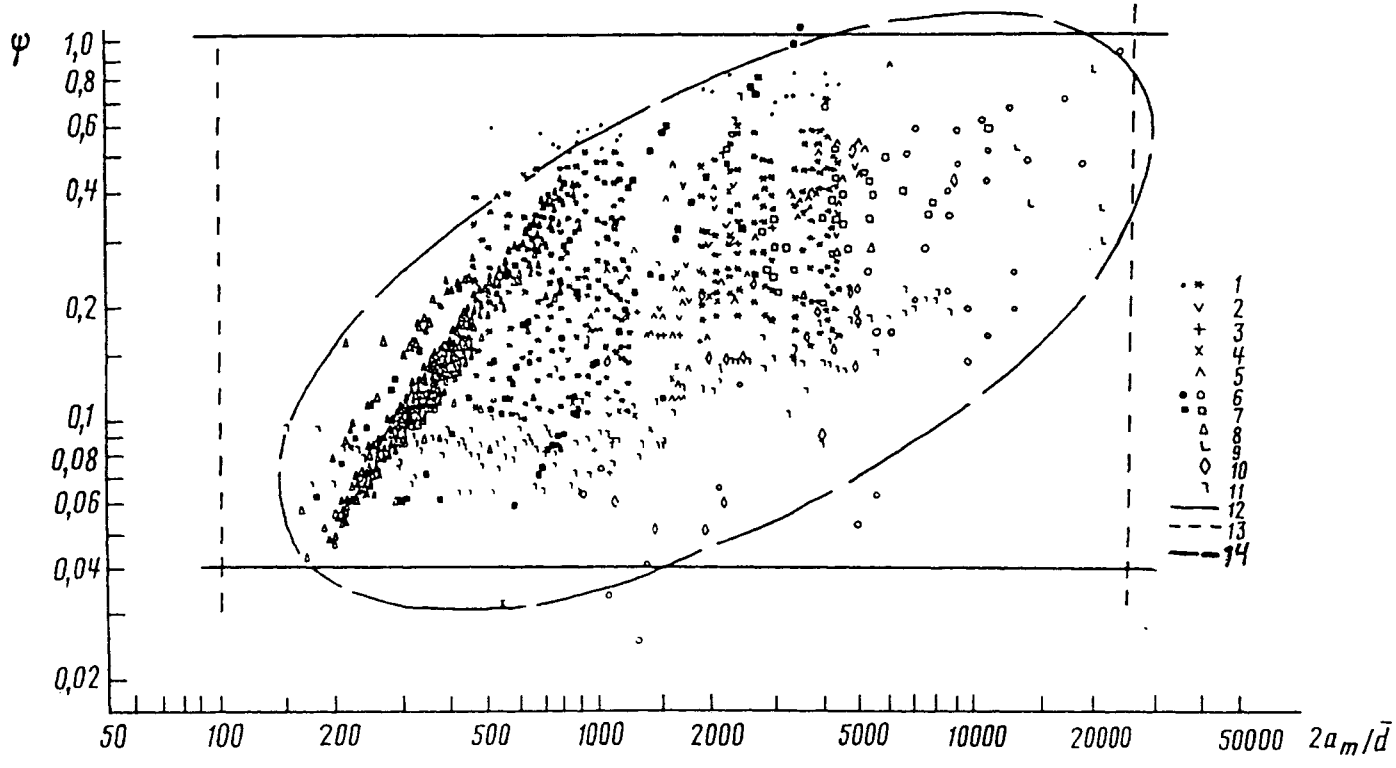

FIGURE 71 An area of wave ripple existence on the basis of experimental data: (1) Manohar, 1955; (2) "Kamchia-78"; (3) "Shkorpilovtzy-82"; (4) "Shkorpilovtzy-83"; (5) "Shkorpilovtzy-85"; (6) Miller and Komar, 1980b; (7) Nielsen, 1984; (8) Keremetchiev (unpublished data); (9) Tanner, 1971; (10) Inman, 1957; (11) Nielsen, 1979; (12) limiting curve after Nielsen, 1979; (13) limiting curve by (5.10).